ELSEVIER

Analytica Chimica Acta 338 (1997) 155–162

ANALYTICA CHIMICA ACTA

Correction of fluorescence inner filter effects and the partitioning of pyrene to dissolved organic carbon

Bruce C. MacDonald[a,*], Sergey J. Lvin[b], Howard Patterson[c]

[a] *Central Research Division, Pfizer Inc., Eastern Point Road, Groton, CT 06340-9979, USA*
[b] *Department of Mathematics and Statistics, University of Maine, Orono, ME 04469-5752, USA*
[c] *Department of Chemistry, University of Maine, Orono, ME 04469-5706, USA*

Received 22 March 1996; revised 18 June 1996; accepted 20 June 1996

Abstract

The ability of dissolved organic carbon (DOC) to bind pyrene can be monitored by fluorescence quenching. Inner filter effects, caused by DOC, complicate the interpretation of the partitioning coefficient of DOC to pyrene. Since DOC absorbs and fluoresces at the excitation wavelength of pyrene, by fitting the DOC self-quenching curve to a simple empirical model that quantifies the absorbance in the spectrofluorimeter's interrogation zone, one can obtain the necessary information to correct for the inner filter effects. This model can be combined with the Stern–Volmer equation to give a single equation that models the total fluorescence of a quenching experiment, and from which a value for the linear Stern–Volmer quenching constant, corrected for the inner filter effects, may be obtained. The mechanisms of inner filter effects are discussed and then quantified, leading to a mathematical model of a self-quenching curve. This is then reduced to the empirical model of DOC self-quenching.

Keywords: Fluorimetry; Inner filter effects; Humic substances; Dissolved organic carbon; Pyrene; Polycyclic aromatic hydrocarbons

1. Introduction

Naturally occurring sources of water contain varying amounts of dissolved organic carbon (DOC), a complex mixture of poorly defined organic and humic acids. Hydrophobic organic pollutants can bind with the hydrophobic regions of DOC, thus altering the fate of the pollutant. Fluorescence quenching and Stern–Volmer plots can be used to determine the partitioning coefficient (K_{sv}) of a polycyclic aromatic hydrocarbon such as pyrene (a model pollutant), to DOC [1–3]. However, the DOC absorption spectrum overlaps the excitation and emission spectrum of the pyrene causing the Stern–Volmer plot to curve upward with increasing DOC concentration. This is a consequence of inner filter effects (IFE) of DOC, and one cannot determine K_{sv}.

In this paper, we present an empirical model of the DOC self-quenching curve. This model contains information that readily allows for the correction of IFE. The model is very similar to a model presented by Kubista et al. [4]. However, their model was applied to primary inner filtering (PIF) only, while the

* Corresponding author.

PII S0003-2670(96)00306-6

models derived in this paper account for both PIF and secondary inner filtering (SIF). It is shown that a rearranged form of the Stern–Volmer equation may be inserted into the empirical model. The resulting model (quenching model) is then fitted to the fluorescence quenching data by nonlinear regression, and a Stern–Volmer quenching constant (K_{sv}) is obtained.

Finally, a mathematical model of fluorescence in the presence of IFE is independently derived. It is shown that the mathematical model may be reduced to the much simpler empirical model. This provides theoretical support for the empirical model. Correction factors from the mathematical model are related to the correction factors derived by Parker and Barnes [5] and Lackowicz [6].

2. Experimental

The DOC used in these experiments was obtained by water extraction of the organic surface layer of a coniferous upland stand in Bradley, Maine. The organic material was lightly packed to fill a 2 l flask, which was then filled with distilled and de-ionized water. After sitting for 6 h, approximately 1 l of a DOC solution was obtained. This was filtered through Gelman A/E glass fiber filters and Gelman Vacucap 0.45 micron filters. The filtrate was passed through a cation exchange column of Rexyn 101 H beads to remove metals, then brought to pH 6 by adding 1 M NaOH. The resulting solution had [DOC]=152 ppm (mg Cl^{-1} of solution).

A concentrated phosphate buffer of pH 6 was prepared by mixing 50 ml of 1.00 M KH_2PO_4 and 5.6 ml of 1.00 M NaOH and then diluting it to 100 ml. Buffered solutions were prepared from this by mixing 1 ml of the concentrated buffer to each of the 49 ml of the solution to be buffered.

A buffered stock of pH 6 aqueous pyrene (6.15×10^{-7} M) was prepared from 2.05×10^{-4} M pyrene in methanol. 1.5 ml of this solution was slowly added to 498.5 ml of buffered water of pH 6.

Fluorescence data was collected on a PTI QM-1 fluorescence spectrometer. The excitation monochromator was set at 334 nm and the emission monochromator was scanned from 370 to 400 nm. Both, the excitation (Δy) and emission (Δx) slits were set at 0.125 cm, which corresponds to a 5 nm band-pass. Absorbance of the DOC dilutions was measured at 334 and 394 nm. This data is presented in Table 1.

Fourteen dilutions of the DOC stock were prepared, ranging from 0 to 152 ppm in concentration. An aliquot of 3.00 ml of each dilution was

Table 1
Absorbance and fluorescence data for DOC solutions

Before pyrene addition				After pyrene addition	
[DOC] ppm	Absorbance at 334 nm	Absorbance at 394 nm	F_{DOC} at 394 nm	DOC ppm	F_{obs} at 394 nm
0.00001 [a]	0.00001 [a]	0.00001 [a]	2321.8	0.00	729460
4.56	0.075	0.0232	92287	4.1455	671200
9.12	0.1452	0.0458	150900	8.2909	637300
13.68	0.2155	0.0657	203300	12.436	596600
18.24	0.2941	0.0956	232100	16.582	576500
27.36	0.4379	0.1377	267300	24.873	507700
36.48	0.5852	0.184	286000	33.164	482300
45.6	0.7355	0.2311	279800	41.455	415700
60.8	0.97	0.3068	245100	55.273	351200
76.0	1.2312	0.3833	209200	69.091	287400
91.2	1.4524	0.4601	169100		
121.6	1.9186	0.6149	107200		
136.8	2.176	0.6931	82346		
152	2.4739	0.7855	61324		

[a] The first sample is for water blank with no DOC. The [DOC] and absorbance values were actually zero. Since the models are undefined at zero, 0.00001 was entered for these parameters.

placed in a cuvette in the spectrofluorimeter and the fluorescence intensity of the DOC was recorded at 394 nm (F_{DOC} at 394 nm in Table 1). Next an aliquot of 0.300 ml of the pyrene stock was added to the cuvette, the contents mixed and the fluorescence intensity at 394 nm was recorded after 4 min after mixing (F_{obs} in Table 1). The DOC fluorescence intensity and the total fluorescence were recorded in this manner for the first 10 dilutions. For the four DOC dilutions remaining, no pyrene was added, and only the fluorescence intensity of DOC was scanned.

3. Results and discussion

3.1. Empirical model of DOC fluorescence

DOC not only absorbs light but also has a very broad emission spectrum. This provides a method for quantifying the degree of inner filtering. The F_{DOC} data in Table 1 was fit to the following model:

$$F_{DOC} = F' \cdot [DOC] \cdot \exp(-f \cdot [DOC]) \quad \text{(empirical model)} \quad (1)$$

by varying F' and f, the best fit was obtained. This resulted in F'=20,500 and f=0.0263 (see Fig. 1).

The fluorescence behavior for increasing DOC concentrations can easily be interpreted from the empirical model. At low concentrations, F_{DOC} is nearly a linear function of F'[DOC]. As the DOC concentration increases, the absorbance of the solution becomes significant, inner filtering increases, and the fluorescence decreases according to the term $\exp(-f\cdot[DOC])$. A correction factor for the self-quenching behavior of DOC is simply the reciprocal of the exponential term

$$\exp(+f \cdot [DOC]) \quad \text{(empirical correction factor)} \quad (2)$$

Note that this inner filter correction factor is obtained without measuring the absorbance or the coordinates of the interrogation zone of the spectrofluorimeter.

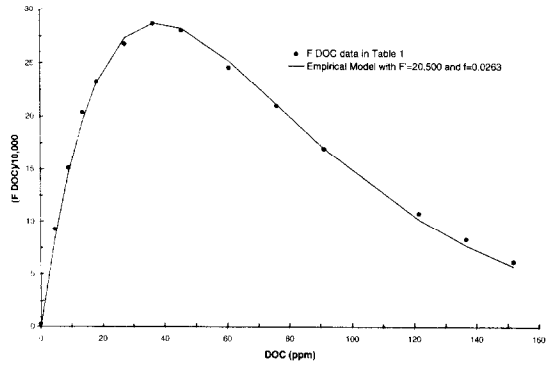

Fig. 1. Empirical model of fluorescence (solid line) fitted to the F_{DOC} fluorescence data in Table 1.

3.2. Determining Stern–Volmer constants

Next, we develop a model for the fluorescence of a DOC–pyrene quenching experiment from which K_{sv} may be obtained, even in the presence of IFE. We begin by supposing a very simple pyrene–DOC quenching experiment; a situation where the DOC contributes no fluorescence and causes no IFE. In this case, the observed fluorescence versus the DOC concentration would be described by:

$$F_{pyr} = \frac{F_0}{1 + K_{sv}[DOC]} \quad (3)$$

This is a simple rearrangement of the Stern–Volmer model. However, as the DOC concentration increases, it does contribute to the observed fluorescence (F_{obs}). Thus, we can write:

$$F_{obs} = \frac{F_0}{1 + K_{sv}[DOC]} + F'[DOC] \quad (4)$$

using F'[DOC] to quantify the fluorescence of the DOC. Finally, the DOC causes IFE as its concentration increases. This diminishes the observed fluorescence of both the pyrene and the DOC. Thus,

$$F_{obs} = \left(\frac{F_0}{1 + K_{sv}[DOC]} + F'[DOC]\right) \cdot \exp(-f \cdot [DOC]) \quad \text{(quenching model)} \quad (5)$$

Eq. (5) models the quenching of pyrene by DOC. Essentially, it is the empirical model of DOC fluorescence containing the Stern–Volmer model within. Fig. 2 summarizes the steps involved in collecting the data and applying the quenching model. Fig. 3 shows the result of the fitting of the quenching model to the F_{obs} data in Table 1 with K_{sv}=0.0206. Since the fit is very good (r^2=0.9967), it

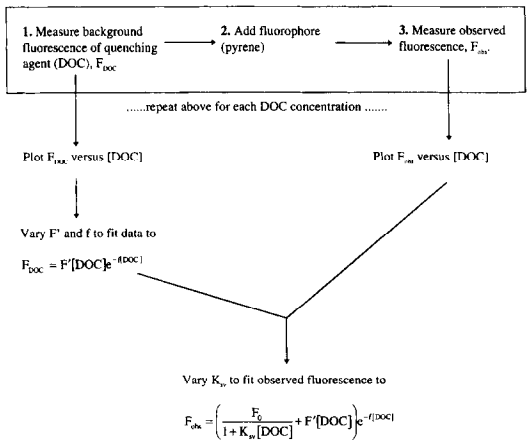

Fig. 2. Flow chart summarizing steps for data collection and application of the quenching model to determine K_{sv}.

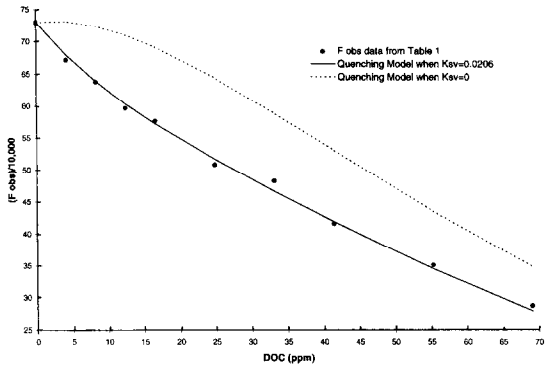

Fig. 3. Quenching model of fluorescence fitted to the F_{obs} data (see Table 1) when K_{sv}=0.0206 (solid line) or when K_{sv}=0 (dashed line).

is reasonable to assume that the linear Stern–Volmer quenching occurs between the DOC and pyrene. Note that this value of K_{sv} was obtained at DOC levels up to 76 ppm. This is a higher level than is typically used by other authors [1,3]. Fig. 3 also shows the output of the quenching model if the pyrene had no affinity for DOC, i.e. if K_{sv} equalled zero.

The correction factors derived above and noted in other publications are typically used first by correcting the data, and then by making the Stern–Volmer plots. This is equivalent to solving the quenching model for the term $1+K_{sv}[DOC]$, and then using the least squares method for determining K_{sv}. Applying these two approaches to the data in this paper shows that the resulting K_{sv} values are nearly identical up to 27 ppm DOC. Thereafter, the method of least squares leads to an underestimation of K_{sv}. It is more accurate to vary K_{sv} in the quenching model to achieve a fit to the F_{obs} data. The alternative approach, solving the quenching model for K_{sv}, defines K_{sv} in terms of a different equation which the fitting algorithm may treat in a different manner while determining K_{sv}. The quenching model and a nonlinear regression algorithm, such as that found in KaleidaGraph [7] or SigmaPlot [8], provide a more accurate estimate of K_{sv} when higher absorbance values are involved.

3.3. Mathematical model of fluorescence with inner filter effects

A significant feature of the quenching model is the empirical model of the DOC self-quenching curve. Here, we wish to derive a mathematical model of fluorescence self-quenching, and relate this to the parameters F' and f of the empirical model.

The fluorescence intensity of a dilute solution of a fluorophore can be expressed as:

$$F = k\phi\Delta y(I_{x1} - I_{x2}) \tag{6}$$

where k is a proportionality constant, ϕ the quantum yield, I_{x1} and I_{x2} are measures of the photon density at points x_1 and x_2 along the light path, and Δy is the width of the excitation slit (see Fig. 4). From Beer's

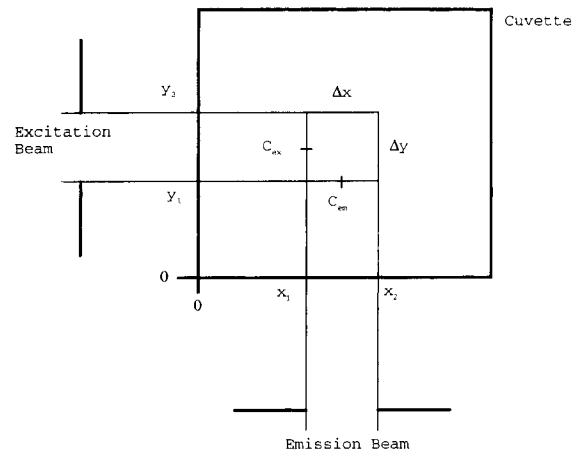

Fig. 4. Cross section of a cuvette showing parameters of the interrogation zone (illustration not to scale).

Law, we have $I_x=I_0\exp(-\alpha_f x)$, where α_f is the product of the fluorophore's extinction coefficient and concentration: a_f and c_f, respectively, and x is the distance traveled through the solution. Substituting Beer's Law into Eq. (6) and rearranging, we get:

$$F = k\phi I_0 \Delta y \exp(-\alpha_f x_1)(1 - \exp(-\alpha_f \Delta x)) \quad (7)$$

where Δx is the slit width of the emission monochromator in cm.

For a very dilute solution, the concentration of the fluorophore approaches zero, thus α_f approaches zero and Eq. (7) may be linearized to the equation for an ideally dilute fluorophore solution,

$$F_{ideal} = k\phi I_0 \alpha_f \Delta x \Delta y \quad (8)$$

Contained within the constant k there is a constant (Δz) for the height of the zone illuminated by the excitation beam and observed by the emission monochromator. Together, $\Delta x\Delta y\Delta z$ form the interrogation zone of the spectrofluorimeter, the actual volume from which the fluorescence data is gathered by the instrument. We also note here that the center of the excitation beam can be written as $C_{ex} = y_1 + \Delta y/2$ (Fig. 4). A corresponding statement can be made for C_{em}, the center of the emission beam.

Eq. (8) is valid for a very dilute fluorophore solution without significant absorption at the excitation or emission wavelength. The density of the excitation photons is essentially uniform throughout the interrogation zone. It follows that any of the fluorophores in the interrogation zone will have an equal probability of absorbing a photon, and each emitted photon has an equal probability of escaping from the cuvette and being observed by the emission monochromator.

Contrast the above to a situation in which IFE takes place. For simplicity we assume a solution which contains a population of only two species: a fluorophore and a chromophore which absorbs at both the excitation and emission wavelengths of the fluorophore. Consider the fate of a fluorophore at the positions A and B in a cell (Fig. 5). At A the excitation beam has a greater distance to travel into the cell to excite the fluorophore. There is an increased chance of absorption of the exciting photon by an intervening chromophore or fluorophore. Thus,

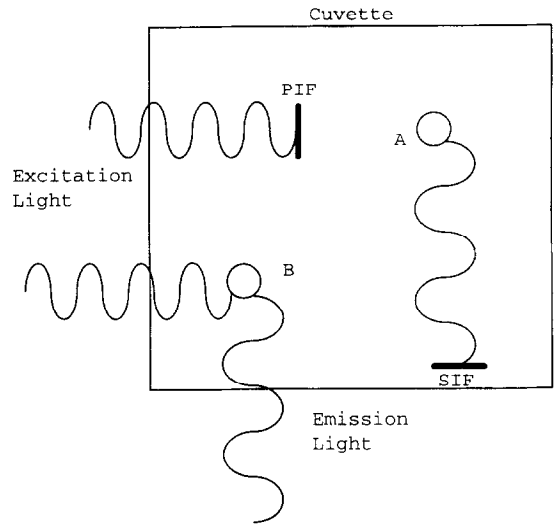

Fig. 5. The mechanisms of inner filter effects (IFE). For a fluorophore located at A, an excitation photon is more likely to be absorbed by an intervening fluorophore or chromophore (primary inner filtering). In the same manner the emitted photon from A is more likely to be absorbed (secondary inner filtering).

the molecule at A is less likely to be observed than the molecule at B. This is the cause of PIF. Similarly, a photon emitted at A is more likely to be absorbed by an intervening chromophore than the photon emitted at B, resulting in SIF. As inner filtering becomes extreme, only the fluorophores in the vicinity of B contribute to the observed fluorescence. Thus, inner filtering occurs when the excitation photon density in the cuvette is not uniform or the probability of an emitted photon being observed by the emission monochromator is not constant for all fluorophores. In other words, the probability of photon absorption or its escape from the cell is dependent on the position of the fluorophore in the cell.

The above situation can be quantitatively dealt with. When PIF exists, Eq. (8) is no longer valid. We define $\alpha_{ex} = a_f c_f + a_c c_c$, where a_c and c_c refer to the extinction coefficient and concentration of the chromophore, respectively. If A_{ex} is the absorbance measured at the fluorophore's excitation wavelength in a 1 cm cuvette, α_{ex} is simply $2.3A_{ex}$. At each point x, the intensity of the excitation beam is $I_x = I_0\exp(-\alpha_{ex}x)$. We assume the other factors in Eq. (8), k, ϕ and α_f remain constant, though under

particular experimental conditions other processes such as dynamic quenching or non-radiative (Forster) energy transfer may occur.

Next, let us divide the interrogation zone into infinitely small segments dx, perpendicular to the excitation beam. Within each infinitely small segment Eq. (8) still holds but with $I_0 \exp(-\alpha_{ex}x)dx$ instead of $I_0\Delta x$. The observed fluorescence is the sum of the fluorescence of these ideal segments. Thus, in the presence of PIF Eq. (8) becomes:

$$F = k\phi I_0 \alpha_f \Delta y \int_{x_1}^{x_1+\Delta x} \exp(-\alpha_{ex}x)dx \tag{9}$$

One can also reach this conclusion if it is seen that the fluorescence is proportional to the excitation photon density (I) and the fluorophore density (α_f). Since the inner filter effect reduces the number of photons according to Beer's law, we may integrate Beer's law over the interrogation zone parameters, to obtain the density of photons at each point in the interrogation zone, which also gives Eq. (9).

Now let us take into account the influence of SIF. We consider a population of randomly distributed fluorophores emitting photons in the interrogation zone. The probability of transmittance to the point y_0 is a function of α_{em} (which is simply $2.3A_{em}$ as measured by an absorption spectrophotometer) and the distance of the fluorophore from y_0. While, the Beer's law is more typically used in determining the fraction of photons that travel from y_0 at the surface of the solution to some point within the solution, y_i, it is the distance and not the direction traveled that is important. That is, the probability of going from y_0 to y_i is the same as the probability of going from y_i to y_0. Thus we again integrate Beer's law to determine the fraction of photons that escape from the cell, but with the new parameter α_{em}, and boundaries y_1 and y_2. Thus we can replace Δy in Eq. (9) and write:

$$F = k\phi I_0 \alpha_f \int_{x_1}^{x_1+\Delta x} \exp(-\alpha_{ex}x)dx \cdot \int_{y_1}^{y_1+\Delta y} \exp(-\alpha_{em}y)dy \tag{10}$$

After integration, an equation that describes the observed fluorescence when both PIF and SIF are occurring can be written as:

$$F_{obs} = k\phi I_0 \alpha_f \exp(-\alpha_{ex}x_1)\left(\frac{1-\exp(-\alpha_{ex}\Delta x)}{\alpha_{ex}}\right) \cdot \exp(-\alpha_{em}y_1)\left(\frac{1-\exp(-\alpha_{em}\Delta y)}{\alpha_{em}}\right) \quad \text{(mathematical model)} \tag{11}$$

Note that this equation can be reduced to Eq. (8) by taking the limits as α_{ex} and α_{em}, the causative agents of PIF and SIF, go to zero.

From the mathematical model a correction factor of IFE is also readily derived. As Brand and Witholt [9] noted during the derivation of a primary correction factor, this can be done by making a ratio of the ideal fluorescence, F_{ideal}, to the observed fluorescence, F_{obs} using Eq. (8). Thus the ratio of the ideal to the observed fluorescence is:

$$\frac{F_{ideal}}{F_{obs}} = (k\phi I_0 \alpha_f \Delta x \Delta y)/ \left(k\phi I_0 \frac{\alpha_f}{\alpha_{ex}} \exp(-\alpha_{ex}x_1)(1-\exp(-\alpha_{ex}\Delta x)) \cdot \frac{\exp(-\alpha_{em}y_1)}{\alpha_{em}}(1-\exp(-\alpha_{cm}\Delta y))\right) \tag{12}$$

Converting it to base 10 and rearranging we obtain,

$$\frac{F_{ideal}}{F_{obs}} = \frac{2.3A_{ex}\Delta x 10^{A_{ex}x_1}}{1-10^{-A_{ex}\Delta x}} \cdot \frac{2.3A_{em}\Delta y 10^{A_{em}y_1}}{1-10^{-A_{em}\Delta y}} \quad \text{(mathematical correction factor)} \tag{13}$$

The first quotient after the equal sign is the primary inner filter correction factor, originally published by Parker and Barnes [5] without derivation. J.F. Holland et al. [10] later published a derivation for the Parker correction factor. Here, both the PIF and the SIF correction factors (the final quotient) are explicitly derived. In contrast to Eq. (2), this correction factor depends on the determination of the absorption of the quenching agent at the excitation and emission values of the fluorophore, and the actual coordinates of the interrogation zone. In practice, it is not easy to determine the latter, limiting the practical utility of Eqs. (11) or Eq. (13).

3.4. Relationship between the mathematical and empirical models

The mathematical model contains a term of the form

$$\exp(-\alpha x_1)\left(\frac{1-\exp(-\alpha\Delta x)}{\alpha}\right) \tag{14}$$

Expanding the exponential term in parentheses gives:

$$\exp(-\alpha x_1)\Delta x\left(1-\frac{\alpha\Delta x}{2}+\frac{(\alpha\Delta x)^2}{6}-\frac{(\alpha\Delta x)^3}{24}+\cdots\right) \tag{15}$$

We can approximate the series within the parentheses in Eq. (15) to:

$$\exp\left(-\frac{\alpha x_1\Delta x}{2}\right)=1-\frac{\alpha\Delta x}{2}+\frac{(\alpha\Delta x)^2}{8}-\frac{(\alpha\Delta x)^3}{48}+\cdots \tag{16}$$

The accuracy of this approximation depends on the difference between the quadratic terms in Eqs. (15) and (16), and the size of $\alpha\Delta x$. We may now write:

$$\Delta x\exp\left(-\left(\alpha x_1+\frac{\alpha\Delta x}{2}\right)\right)\approx\Delta x\exp(-\alpha C_{ex}) \tag{17}$$

where $C_{ex}=\alpha x_1+\alpha\Delta x/2$. After treating both exponential terms in the mathematical model as above, we observe that:

$$\exp(-\alpha_{ex}x_1)\left(\frac{1-\exp(-\alpha_{ex}\Delta x)}{\alpha_{ex}}\right)\exp(-\alpha_{em}y_1)\left(\frac{1-\exp(-\alpha_{em}\Delta y}{\alpha_{em}}\right)\approx\Delta x\Delta y\exp(-(\alpha_{ex}C_{ex}+\alpha_{em}C_{em})) \tag{18}$$

This reduces the four exponential terms of the mathematical model to a single exponential term.

For a particular source of DOC, a certain fraction of it behaves as a fluorophore or as a chromophore (p_f and p_c, respectively). We can express the concentration of the fluorophore as $c_f=p_f[DOC]$. Using this relationship and the right side of Eq. (18), we can write Eq. (11) as

$$F_{DOC}=k\phi I_0\Delta x\Delta y a_f p_f[DOC]\cdot\exp(-(\alpha_{ex}C_{ex}+\alpha_{em}C_{em})) \tag{19}$$

Eq. (19) can also provide a definition of the parameters in the value of f for the empirical model. Let us assume for simplicity of notation that the DOC solution contains only one fluorophore and one chromophore species, with absorptivities and concentrations a_f, c_f and a_c, c_c, respectively. We assume the fluorophore absorbs only at the excitation wavelength and the chromophore absorbs only at the emission wavelength. We then use $c_f=p_f[DOC]$ and $c_c=p_c[DOC]$ as the fractions of the total DOC concentration, which are made of fluorophore and chromophore, respectively, and rewrite the exponential term of Eq. (19) as:

$$\exp(-(\alpha_{ex}C_{ex}+\alpha_{em}C_{em}))=\exp(-(a_f p_f C_{ex}+a_c p_c C_{em})[DOC]) \tag{20}$$

We can now combine the information in Eqs. (19) and (20) and write

$$F=k\phi I_0\Delta x\Delta y a_f p_f[DOC]\exp(-(a_f p_f C_{ex}+a_c p_c C_{em})[DOC]) \tag{21}$$

Eqs. (14)–(21) show that the mathematical model may be reduced to the empirical model where $F'=k\phi I_0\Delta x\Delta y a_f p_f$, f being a constant dependent on the extinction coefficient and fractional abundance of each of the absorbing species. All the equations and parameters in this paper may be modelled and defined on a spreadsheet. At low absorbance values F' or f can be calculated directly from the parameters in Eq. (21). When the absorbance is high these parameters cannot be accurately derived from the mathematical model (due to the approximation in Eq. (17)) unless a fitting factor is introduced. However, it should be clear that this approximation does not affect the accuracy of the empirical model in modeling F_{DOC}.

The exponential term of Eq. (19) can also be related to a correction factor provided by Lackowicz [6] for IFE. If the alignment of the spectrofluorimeter is such that C_{ex} and C_{em} equal 0.5 cm, we see that the exponential term in Eq. (19) is simply half of the sum of the absorbancies at the excitation and emission

wavelengths. Lackowicz presented exactly this as an approximate correction factor. The arguments above show it to be a very precise correction factor when $C_{ex}=C_{em}=0.5$ and the absorbance is not high. Also, when the concentration of the species absorbing at the emission wavelength is zero, the correction factor for Eq. (19) reduces to the correction factor provided by Kubista et al. [4]. Finally, Eq. (19) can be used in an IFE correction method, where the cuvette is moved and thus C_{ex} and C_{em} become variables.

4. Conclusion

The empirical model quantifies the fluorescence intensity of DOC and the degree of inner filtering based on single variable of DOC concentration and two constants. The two constants are determined for each source of DOC by fitting the empirical model to a plot of the fluorescence intensity versus concentration of the various DOC dilutions (F_{DOC}) used in the quenching experiment.

A mathematical model for fluorescence with inner filter effects is independently derived from Beer's law. This model requires that the coordinates of the spectrofluorimeter's interrogation zone and the absorbance of the DOC solutions at the excitation and emission wavelengths be known. The simpler empirical model is actually an approximation of the more complicated mathematical model.

In a quenching experiment between DOC and pyrene, the total observed fluorescence, F_{obs}, is a result of three sources: (1) the pyrene–DOC quenching, (2) the F_{DOC}, and (3) the inner filter effects of DOC. The Stern–Volmer model can be used to quantify the first source while the empirical model most easily quantifies the last two sources. The Stern–Volmer and the empirical models can be combined and fit to the F_{obs} data of the quenching experiment by varying K_{sv}. If the fit conforms to the data, one will obtain an accurate value of K_{sv}. This method allows the determination of K_{sv} at DOC concentrations which are higher than typically used.

The approach used in obtaining the empirical model of the DOC self-quenching curve may be applied to other quenching agents that fluoresce and absorb at the excitation or emission wavelengths of fluorophore being employed.

Acknowledgements

The authors wish to thank the Maine Water Resources Program and the United States Geological Survey, Department of the Interior for Financial Assistance (USG grant number 14-08-001-G2023).

References

[1] T.D. Gauthier, E.C. Shane, W.F. Guerin, W.R. Seitz and C.L. Grant, Environ. Sci. Technol., 20 (1986) 1162.
[2] D.A. Backhus and P.M. Gschwend, Environ. Sci. Technol., 24 (1990) 1214.
[3] M.M. Puchalski, M.J. Morra and R.V. Wandruszka, Environ. Sci. Technol., 26 (1992) 1787.
[4] M. Kubista, R. Sjoback, S. Erickson and B. Albinsson, Analyst, 119 (1994) 417.
[5] C.A. Parker and W.J. Barnes, Analyst, 82 (1957) 606.
[6] J.R. Lackowicz, Principles of Fluorescence Spectroscopy, Plenum Press, New York. 1983, p. 45.
[7] KaleidaGraph, Ablebeck Software, Version 3.0.1, 1993.
[8] SigmaPlot, Jandel Corporation, Version 2.01, 1994.
[9] L. Brand and B. Witholt, Methods of Enzymology, 1967, p. 776.
[10] J.F. Holland, R.E. Teets, P.M. Kelly and A. Timnick, Anal. Chem., 49 (1977) 706.